AIP | Journal of Applied Physics

Experimental verification of intermediate band formation on titanium-implanted silicon

H. Castán, E. Pérez, H. García, S. Dueñas, L. Bailón et al.

Citation: J. Appl. Phys. **113**, 024104 (2013); doi: 10.1063/1.4774241
View online: http://dx.doi.org/10.1063/1.4774241
View Table of Contents: http://jap.aip.org/resource/1/JAPIAU/v113/i2
Published by the American Institute of Physics.

Experimental verification of intermediate band formation on titanium-implanted silicon

H. Castán,[1,a)] E. Pérez,[1] H. García,[1] S. Dueñas,[1] L. Bailón,[1] J. Olea,[2,3] D. Pastor,[2,3,4] E. García-Hemme,[2,4] M. Irigoyen,[2,4] and G. González-Díaz[2,4]
[1]*Dept. de Electricidad y Electrónica, Universidad de Valladolid, ETSI Telecomunicación, Paseo de Belén 15, 47011 Valladolid, Spain*
[2]*CEI Campus Moncloa, UCM-UPM, Madrid, Spain*
[3]*Instituto de Energía Solar, E.T.S.I. de Telecomunicación, Universidad Politécnica de Madrid, 28040 Madrid, Spain*
[4]*Dept. de Física Aplicada III (Electricidad y Electrónica), Facultad de Ciencias Físicas, Universidad Complutense de Madrid, Av. Complutense s/n, 28040 Madrid, Spain*

(Received 6 August 2012; accepted 17 December 2012; published online 10 January 2013)

Intermediate band formation on silicon layers for solar cell applications was achieved by titanium implantation and laser annealing. A two-layer heterogeneous system, formed by the implanted layer and by the un-implanted substrate, was formed. In this work, we present for the first time electrical characterization results which show that recombination is suppressed when the Ti concentration is high enough to overcome the Mott limit, in agreement with the intermediate band theory. Clear differences have been observed between samples implanted with doses under or over the Mott limit. Samples implanted under the Mott limit have capacitance values much lower than the un-implanted ones as corresponds to a highly doped semiconductor Schottky junction. However, when the Mott limit is surpassed, the samples have much higher capacitance, revealing that the intermediate band is formed. The capacitance increasing is due to the big amount of charge trapped at the intermediate band, even at low temperatures. Ti deep levels have been measured by admittance spectroscopy. These deep levels are located at energies which vary from 0.20 to 0.28 eV below the conduction band for implantation doses in the range 10^{13}-10^{14} at./cm^2. For doses over the Mott limit, the implanted atoms become nonrecombinant. Capacitance voltage transient technique measurements prove that the fabricated devices consist of two-layers, in which the implanted layer and the substrate behave as an n^+/n junction. © *2013 American Institute of Physics*. [http://dx.doi.org/10.1063/1.4774241]

I. INTRODUCTION

The formation of an intermediate band (IB) in the mid gap of a semiconductor has shown potential for drastically improving the efficiency of single junction solar cells.[1] This approach enable electrons with energy lower than the semiconductor band gap to be pumped from the valence band into conduction band via two-photon absorption of lower energy that use this IB as a midway step. So, single junction solar cells based on a semiconductor with an IB could reach efficiency values well above the maximum theoretical efficiency for single junction cells[2] and also much higher than those obtained on multijunction, multilayer solar cells.[3] IB solar cells can be created in a semiconductor from deep level impurities if their concentration is high enough. Detection of an IB in several semiconductors such as GaNAsP,[4] ZnMnOTe,[5] and GaInNAs,[6] by using optical characterization techniques has been reported.

Ti is a well-known impurity which introduces a deep donor level in the upper half of the silicon band gap. For instance, a level at 0.22 eV below the conduction band has been detected by Hall effect experiments.[7] However, deep level transient spectroscopy studies pointed to a deeper position of the level about 0.29 eV.[8] It is suggested that Ti atoms diffuse in Si through a simple interstitial process according to electron paramagnetic resonance measurements.[9] These impurities are a well-known source of non-radiative Shockley-Reed-Hall (SRH) recombination. However, it has been argued that this recombination may be suppressed when the Ti concentration is high enough as to exceed the Mott transition (5×10^{19} cm^{-3}). At these high concentrations, a continuous energy band is formed, instead of isolated single-energy level impurities.[10]

It has been proved that the combination of different processing techniques and the use of laser thermal processing allow the introduction of Ti atoms into the Si lattice in concentrations near or above the Mott limit, proving the possibility to form the IB in Si with this element.[11]

In a recent paper, Garcia-Hemme *et al.*[12] have analyzed the increase of the sheet conductance under spectral illumination in high dose Ti implanted Si samples subsequently processed by pulsed-laser melting. Samples with Ti concentration clearly above the insulator-metal transition limit show a remarkably high sheet conductance, even higher than that measured in a silicon reference sample. This increase in the conductance magnitude is contrary to the classic understanding of recombination centers action and supports the

[a)]Author to whom correspondence should be addressed. Electronic mail: helena@ele.uva.es.

lifetime recovery predicted for concentrations of deep levels above the insulator-metal transition.

In this work, we use samples obtained in this way to prove the formation of intermediate band on Si by means of electrical characterization. Results obtained by capacitance measurements, admittance spectroscopy, and capacitance-voltage transient technique (CVTT) show the existence of active Ti deep levels and evidence the formation of the intermediate band.

II. SAMPLE FABRICATION

300 μm Si (111) n-type samples ($\mu = 1450$ cm^2/Vs; $n = 2.2 \times 10^{13}$ cm^{-3} at room temperature) were implanted in an ion beam service (IBS) refurbished VARIAN CF3000 Ion Implanter at 32 KeV with Ti at high doses (10^{13}, 10^{14}, and 10^{16} cm^{-2}). Then, the implanted Si samples were annealed by means of the pulsed laser melting (PLM) method to recover the crystal lattice.[12] The combination of two highly non-equilibrium techniques (ion implantation and subsequent PLM treatment) allows us to build up a new class of semiconductors that avoid equilibrium constraints.[13] The PLM annealing process was performed by J. P. Sercel Associates Inc. (New Hampshire, USA). Samples were annealed with one 20 ns long pulse of a KrF excimer laser (248 nm) at energy density of 0.6–0.8 J/cm^2. PLM is a highly non-equilibrium processing technique which is able to melt and recrystallize the Si surface up to about 100 nm deep in very short times (10^{-8}-10^{-6} s). This rapid recrystallization time allows the incorporation of Ti atoms to the Si at concentrations well above the solubility limit for this element. Also, the PLM processing of the Ti implanted Si layer prevents secondary phase formation (i.e., Ti silicide) even when the equilibrium solubility limit has been greatly exceeded. Bottom and top electrodes were fabricated by aluminum evaporation. To obtain good ohmic contacts on the bottom, n^+ layer were fabricated on the back side of the samples (substrate) by ion implantation of phosphorous in a dose of 10^{15} cm^{-2} at energy of 80 keV. Afterwards, samples were annealed at 900 °C during 20 s. Schottky contacts were fabricated in the top just by aluminum evaporation.

Table I summarizes the samples fabrication process. Samples implanted at 10^{13} or 10^{14} cm^{-2} doses have Ti profiles below the Mott limit at any depth. In contrast, sample implanted at 10^{16} cm^{-2} dose shows impurity concentrations beyond the Mott limit up to a depth of 80 nm.

III. EXPERIMENTAL RESULTS

A. Capacitance–voltage measurements

Clear differences exist between the capacitance-voltage behavior of samples implanted with doses under or beyond the Mott limit. Figure 1 shows 10 kHz-capacitance-voltage curves measured at low temperature (77 K) for the three different implantation doses and a non-implanted substrate that will act as reference. Samples implanted under the Mott limit have capacitance values much lower than the non-implanted one as corresponds to a metal-highly doped semiconductor Schottky junction. However, samples implanted beyond the Mott limit exhibit much higher capacitance values due to the big amount of charge trapped at the intermediate band, even at low temperatures.

As ion implantation dose increases, Si is more doped yielding a lowering of the Schottky barrier. In consequence, the capacitance value decreases. For doses beyond the Mott limit, the Fermi level is pinned at the intermediate band, and a new barrier appears between the implanted and non-implanted regions, and the total capacitance increases up to values much higher that for the non-implanted sample.

TABLE I. Samples description.

Sample	Ti implanted dose (at./cm^2)	PL annealing
Witness	None	No
UM1	10^{13} (Under Mott limit)	Yes
UM2	10^{14} (Under Mott limit)	Yes
OM	10^{16} (Over Mott limit)	Yes

B. Admittance spectroscopy

Thermal admittance spectroscopy[14] is a technique which yields thermal emission rates of deep levels from the variations of capacitance and conductance of a p-n or Schottky junction as a function of temperature and frequency. These variations are due to the change in frequency of the measuring signal with respect to the time constant of charge and discharge processes of the deep levels. Measurements consist of recording the capacitance and conductance variation of a bipolar junction as a function of temperature at a given frequency. Each deep level existing in the semiconductor band gap contributes with a peak in the conductance signal and with an inflection point in the capacitance signal. Figure 2 summarizes the results obtained for all the samples studied in this work. We see that samples implanted under the Mott limit (UM1 and UM2) show conductance peaks and capacitance steps as correspond to the deep levels created by the implanted Ti species, whereas non-implanted and over Mott (OM) limit implanted samples do not exhibit any deep level finger print. The fact that OM sample does not exhibit typical deep level admittance spectra agrees with the IB theory,[10] which predicts that deep levels become nonrecombinant

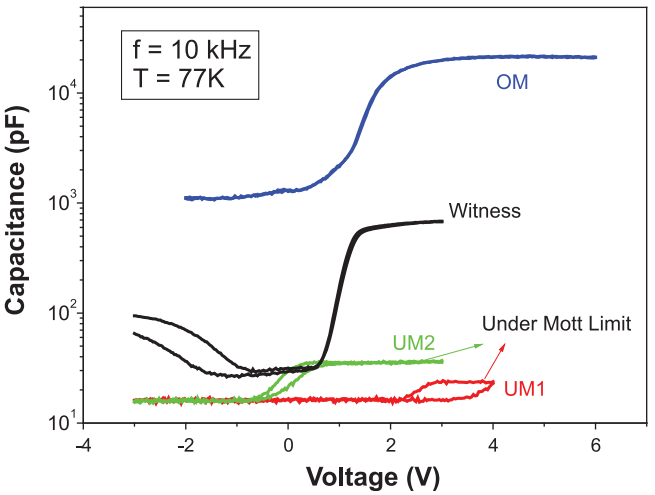

FIG. 1. 10 kHz-capacitance-voltage curves measured at 77 K.

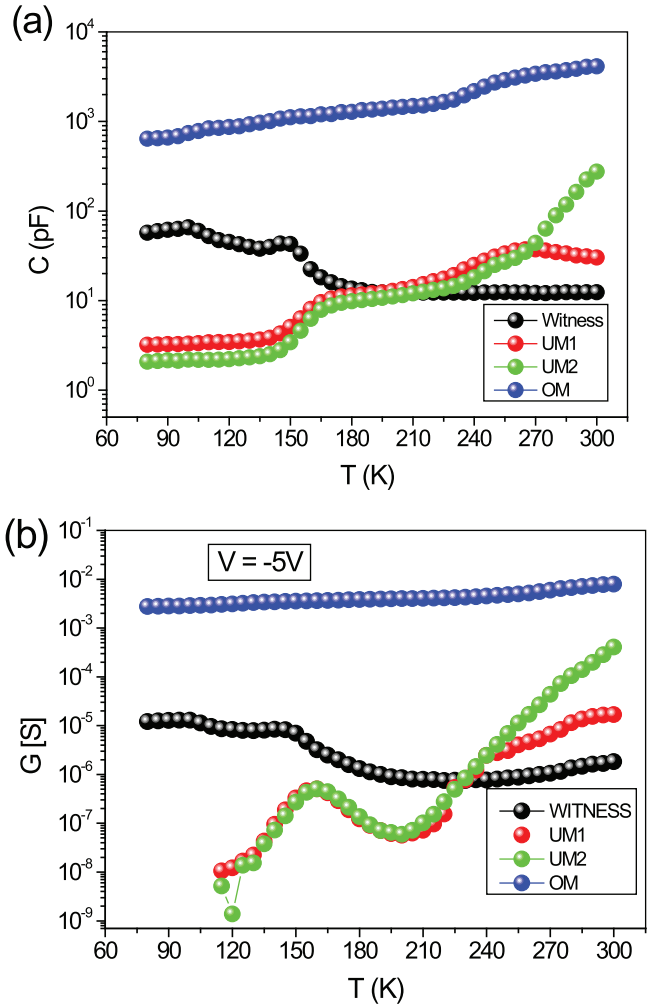

FIG. 2. 30 kHz-capacitance (a) and conductance (b) curves as a function of temperature. Reverse bias was 5 V.

when IB band is formed. This is the first experimental evidence confirming that recombination is suppressed when the Ti concentration is high enough as to exceed the Mott limit.

In Fig. 2, we can see that the conductance peak amplitude is the same for samples implanted at 10^{13} or 10^{14} cm^2 dose. That suggests that the concentration of recombinant deep levels reaches a saturation value. The remaining implanted atoms have a no recombinant nature. This nature becomes dominant when Mott transition occurs.

The conductance peak temperature is related to the deep level emission rate by the well-known equation

$$e_n(T_{peak}) = {}^{\omega}/_{1.98}, \tag{1}$$

where ω is the angular frequency. The emission rate follows an Arrhenius plot law, from which the energy location of the Ti deep level can be obtained. Figures 3 and 4 show the results obtained in this way for samples UM1 and UM2.

Although the deep level energy is in the range of those elsewhere reported,[7,8] it varies depending on the implantation doses. Deep levels are located at 205 meV under the conduction band for samples implanted at 10^{13} cm^{-2}, whereas it reaches a deeper value (278 meV) for samples implanted at 10^{14} cm^{-2}. To summarize the admittance

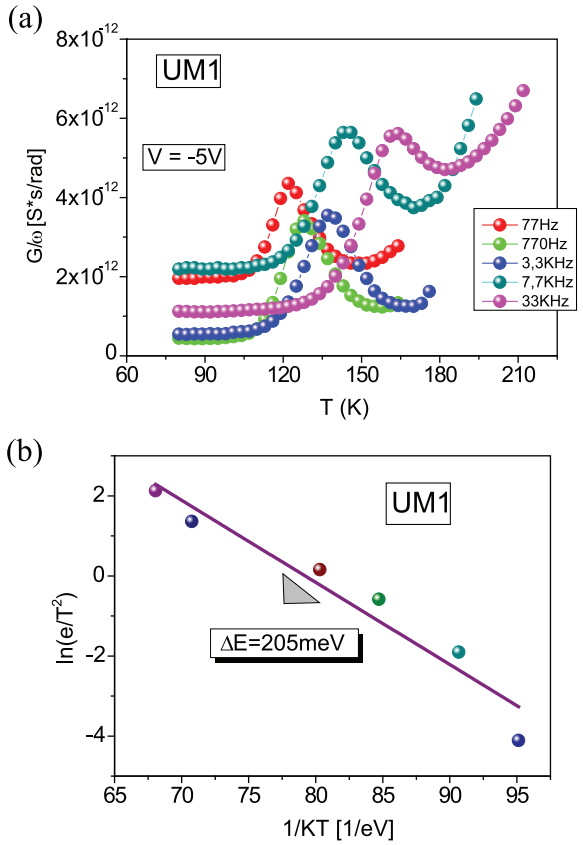

FIG. 3. Admittance spectroscopy results for a sample implanted at 10^{13} cm^{-2}: (a) Conductance vs. temperature at reverse bias of 5 V. (b) Arrhenius plot.

results, we can say that recombinant Ti deep levels trend to be located at deeper energy when the implantation dose increases, but keeping constant its concentration.

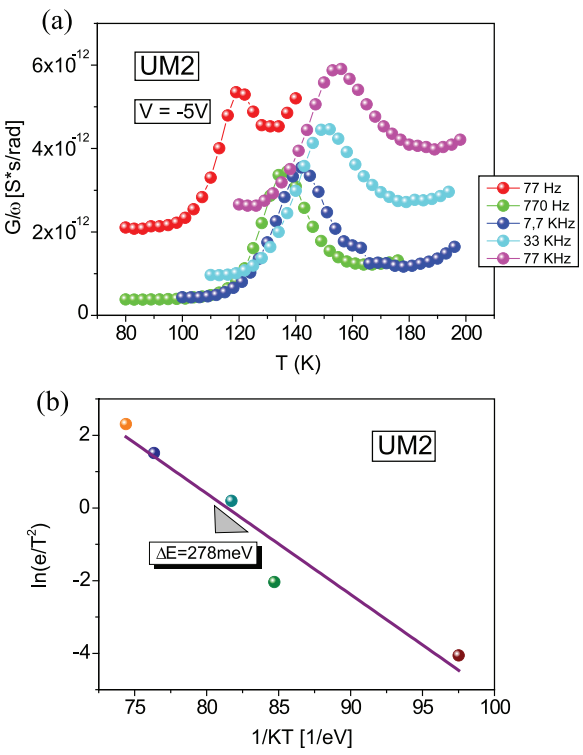

FIG. 4. Admittance spectroscopy results for a sample implanted at 10^{14} cm^{-2}: (a) Conductance vs. temperature at reverse bias of 5 V. (b) Arrhenius plot.

In a previous work, Olea *et al.*[15] proposed for OM sample an analytical two-layer model, in which the implanted layer and the substrate behave as an IB/n-Si type junction. They also deduce that the IB is located at 0.38 eV below the conduction band and carriers at the IB behave as holes with a mobility of 0.4–0.6 $cm^2\ V^{-1}\ s^{-1}$. This deeper energy value agrees with the trend of deep levels to reach deeper energies as doses increase.

C. CVTT

Among the different techniques used to determine doping profiles in semiconductors, the C-V technique is one of the most extensively used. The main advantage of C-V is to be a non-destructive technique, just like photovoltage spectroscopy and unlike other techniques such as spreading-resistance or Hall-effect based techniques. Moreover, C-V technique has a greater sensitivity than other techniques. In a previous work,[16] we presented a technique based on C-V measurements that allows one to obtain both the profiles and emission activation energies for all deep centers present in the junction. This technique, named the CVTT, consists of recording the instantaneous C-V curve just after an emission pulse is applied to the junction. The experimental set-up is basically the same as for standard C-V but it shows some important differences. The reverse bias consists of pulses whose duration is scanned in order to modify the time in which the deep levels are emitting. The fall edge of these pulses is non-abrupt but it is ramp like. The fall time of the ramp is chosen to be very much lower than the emission time constants of the deep levels. Thus, from the view point of the emission process, the ramp can be considered as instantaneous, with no emission taking place during it.

A simplified expression of CVTT can be obtained from Ref. 16 for the case in which only one deep level exists in the semiconductor:

$$\frac{dV_R}{dC} = -\frac{q\varepsilon_0\varepsilon_s A^2}{C^3}\left[N_A(w) + N_T(w)\left(1 - e^{-e_n t_{em}}\right)\right] \quad , \qquad (2)$$

where e_n is the deep level emission rate, V_R is the reverse voltage, C is the capacitance, w is the junction space charge region thickness, and N_A(w) and $N_T(w)$ are, respectively, the densities of shallow impurities and deep levels at the limit of the space charge region.

We obtained CVTT transients for UM1 and UM2 samples, but these transients did not appear for over Mott implanted samples since implanted species become non recombinant. Figure 5 illustrates CVTT transients for the 10^{14} at./cm^2 implanted sample. Figures 5(a) and 5(b) correspond to temperatures in the range where conductance peaks occur. We can see that the amplitude of the capacitance transients increases as the duration of the emission pulse previous to the voltage ramp tends to zero. This is the usual

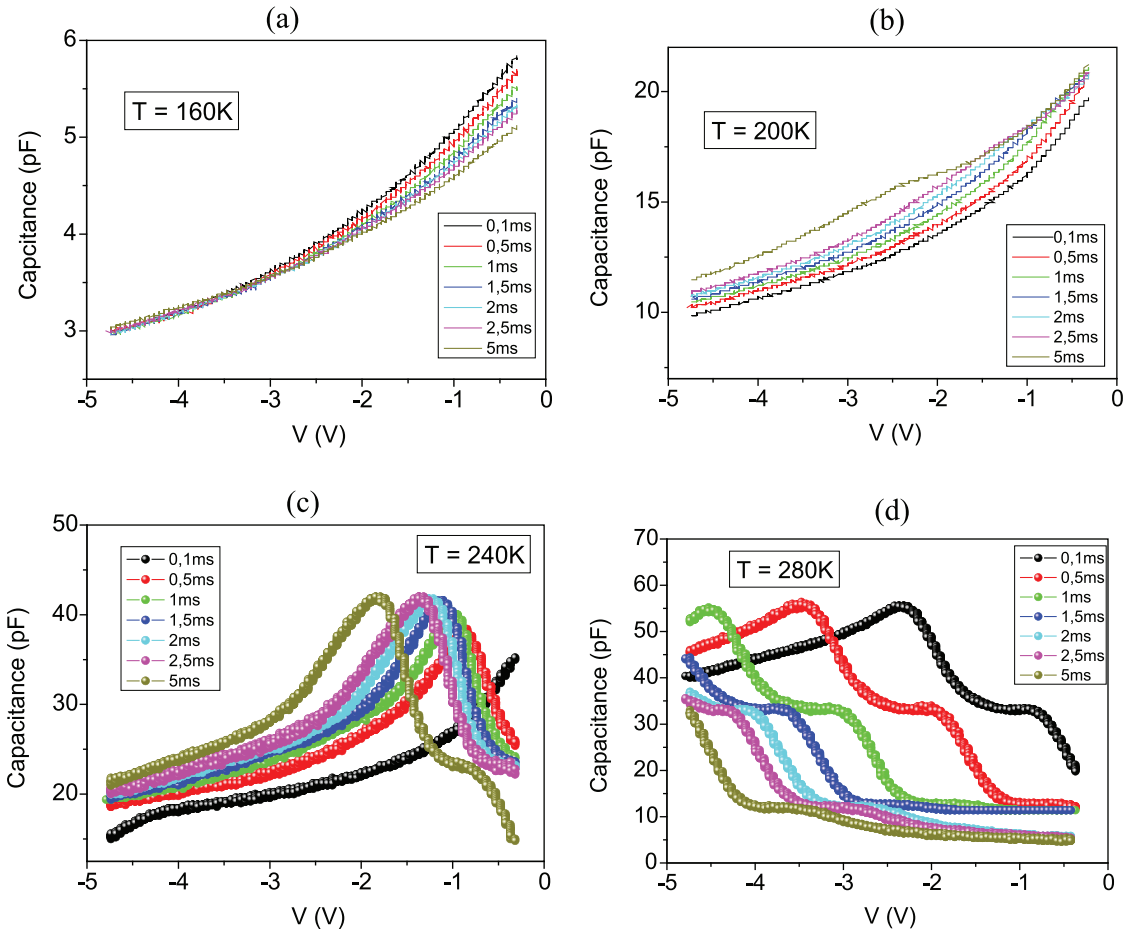

FIG. 5. 1 MHz-CVTT curves at several temperatures corresponding to a sample implanted at $10^{14}\ cm^{-2}$.

behavior for a typical deep level. However, at higher temperatures, the transients are very anomalous. At 240 K, a peak appears which moves towards more negative voltage as the emission pulse duration increases. This fact is more pronounced at room temperature (280 K). That can be explained in terms of the model proposed by Olea *et al.*[15] There are two types of charges: negative charge due to electrons at the conduction band and positive charge due to holes at the intermediate band that begins to be formed in the under Mott samples. In consequence, the implanted substrate shows a hybrid behavior of n-type and p-type (due to IB) substrate at the same time. However, that is not the case for samples implanted under the Mott limit. For these, the implanted layer is just a highly doped semiconductor with a high deep level concentration. The entire device can be modeled as a Schottky diode in series with a n^+/n homojunction (Fig. 6). The Schottky diode is the one formed by the top metal and the implanted semiconductor layer. The n^+/n junction is formed by the highly doped n-type implanted layer and the non-implanted substrate. When a negative voltage is applied between top and bottom electrode, the Schottky diode is reversely biased and its capacitance, C_S, decreases with voltage. In contrast, a forward voltage is applied to the n^+/n junction and its capacitance, C_J, increases with voltage. The measured capacitance results from the composition of the two in series capacitances

$$C_M^{-1} = C_S^{-1} + C_J^{-1} \tag{3}$$

and its value is determined by the lowest of the two capacitances. Then, C_S is dominant for the most negative voltages, whereas at low voltages, C_M is determined by C_J. A maximum on the measured capacitance appears that indicates the transition from the C_S-dominated to the C_J-dominated regime. In Figs. 5(c) and 5(d), we can see that the transition peak varies with temperature and the emission pulse duration, t_{em}. At 240 K, C_S dominates for voltages over 2 V with a little t_{em} dependency. At 280 K, this dependency is much more pronounced. That can be easily explained keeping in mind that deep level emission is thermally activated. As temperature increases, the emission rate of deep levels at the implanted region quickly increases. For the same value of t_{em}, a bigger amount of emptied deep levels exists at 280 K than at 240 K. The emitted charge yields much higher values of C_S and shifts the transition peak to higher voltages. At a given temperature, the longer the time while deep levels are emitting, the greater the emitted charge and, i.e., the transition peak moves to higher voltages. Moreover, the total voltage is differently shared between the two junctions: when C_S increases the voltage drop on the n^+/n junction also increases. That is the reason why in Figs. 5(c) and 5(d), the experimental curves seem to move with the emission time while preserving the same shape at the right side of the transition peak. That is an artifact due to the increase of the voltage drop on the *pseudo* p-n junction when emission time increases. To understand this argument, let us see Figure 5 in detail. At low emission times and low temperatures, titanium deep centers have not emitted electrons and remain neutral. Therefore, the impurity concentration in the implanted area (union Schottky) is practically equal to the existing in the non-implanted substrate and the device behaves like a normal Schootky junction (Figures 5(a) and 5(b)). At high temperatures and high emission times, the deep centers are completely ionized and, then, the density of donor impurities ($N_{Ti}^+ + N_D^+$) increases is far superior than the existing in the not implanted substrate, and the device will behave as a reverse junction (Schottky) with a much higher capacitance than the directly biased n^+-n. That is the case of the curve at 5 ms on Figure 5(d). The result is an increasing C-V. At intermediate temperatures and emission times, mixed behavior takes place.

It is important to emphasize that his behavior does not appear for samples implanted over the Mott limit. In fact, samples over the Mott limit show CV curves in which the capacitance does not vary with voltage. The character metallic of the implanted layer makes the device to be like a passive capacitor, as can be seen in Figure 7.

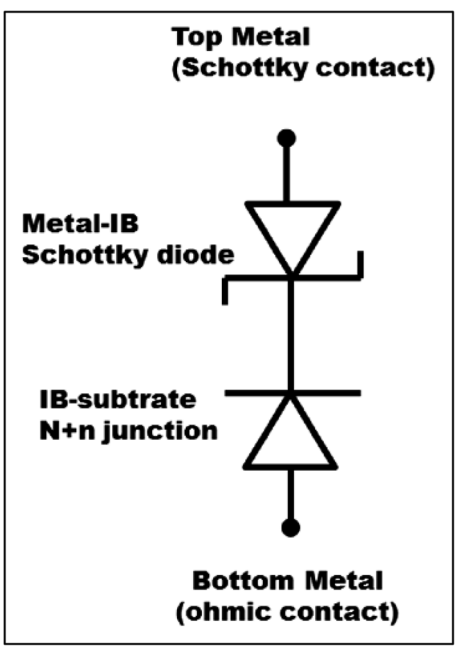

FIG. 6. Circuit model for the under-Mott implanted samples.

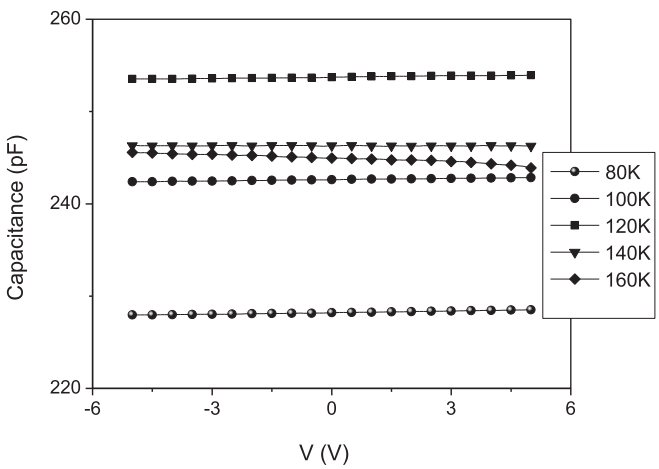

FIG. 7. Capacitance-voltage curves at several temperatures for an over-Mott implanted sample.

IV. CONCLUSIONS

Intermediate band on silicon layers for solar cell applications was achieved by titanium implantation and laser annealing. A two-layer heterogeneous system, formed by the implanted layer and by the un-implanted substrate, was obtained. C-V measurements show clear differences between samples implanted with doses under or beyond the Mott limit.

Admittance spectroscopy results evidence that when Ti implantation overcomes the Mott limit, the deep centers do not show conductance peaks. This is the first experimental evidence confirming that recombination is suppressed when the Ti concentration is high enough as to exceed the Mott limit. Conductance peak amplitude is the same for samples implanted at 10^{13} or 10^{14} cm^{-2} dose. That suggests that the concentration of recombinant deep levels reaches a saturation value. The remaining implanted atoms have a no recombinant nature. This nature is dominant when Mott transition occurs. Deep levels are located at 205 meV under the conduction band for samples implanted at 10^{13} cm^{-2}, whereas it reaches a deeper value (278 meV) for the 10^{14} at./cm^{-2} implantation dose.

CVTT transients are not obtained for samples beyond the Mott limit. CVTT measurements on samples under the Mott limit show a peculiar behavior which allows these devices to be modeled as a Schottky junction in series with an n^+/n homojunction.

ACKNOWLEDGMENTS

This work was partially supported by VA128A11-2 funded by the Junta de Castilla y León and the Spanish TEC2011 under Grant 27292-C02-01, CSD2006-00004 funded by the Spanish Consolider National Program and the Project NUMANCIA II (Grant No. S-2009/ENE/1477) funded by the Comunidad de Madrid. Research of E. Perez was supported by a University of Valladolid FPI grant and research of E. Garcia-Hemme by a PICATA predoctoral fellowship of the Moncloa Campus of International Excellence (UCM-UPM).

Authors would like to acknowledge the CAI de Técnicas Físicas of the Universidad Complutense de Madrid for the ion implantations and metallic evaporations. J. Olea and D. Pastor thank Professor A. Martí and Professor A. Luque for useful discussions and guidance and acknowledge financial support from the MICINN within the program Juan de la Cierva (JCI-2011-10402 and JCI-2011-11471), under which this research was undertaken.

[1]A. Luque and A. Martí, Phys. Rev. Lett. **78**, 5014 (1997).
[2]W. Shockley and H. J. Queisser, J. Appl. Phys. **32**, 510–519 (1961).
[3]R. R. King, D. C. Law, K. M. Edmondson, C. M. Fetzer, G. S. Kinsey, H. Yoon, R. A. Sherif, and N. H. Karam, Appl. Phys. Lett. **90**, 183516 (2007).
[4]K. M. Yu, W. Walukiewicz, J. W. Ager, D. Bour, R. Farshchi, O. D. Dubon, S. X. Li, D. Sharp, and E. E. Haller, Appl. Phys. Lett. **88**, 092110 (2006).
[5]K. M. Yu, W. Walukiewicz, J. Wu, W. Shan, J. W. Beeman, M. A. Scarpulla, O. D. Dubon, and P. Becla, Phys. Rev. Lett. **91**, 246403 (2003).
[6]W. Shan, W. Walukiewicz, J. W. Ager, E. E. Haller, J. F. Geisz, D. J. Friedman, J. M. Olson, and S. R. Kurtz, Phys. Rev. Lett. **82**, 1221–1224 (1999).
[7]J.-W. Chen, A. G. Milnes, and A. Rohatgi, Solid-State Electron. **22**, 801 (1979).
[8]D. Mathiot and S. Hocine, J. Appl. Phys. **66**, 5862 (1989).
[9]S. Hocine and D. Mathiot, Appl. Phys. Lett. **53**, 1269 (1988).
[10]A. Luque, A. Martí, E. Antolín, and C. Tablero, Physica B **382**, 320 (2006).
[11]J. Olea, M. Toledano-Luque, D. Pastor, G. González-Díaz, and I. Mártil, J. Appl. Phys. **104**, 016105 (2008).
[12]C. W. White, S. R. Wilson, B. R. Appleton, and F. W. Young, J. Appl. Phys. **51**, 738 (1980).
[13]C. W. White, J. Narayan, and R. T. Young, Science **204**, 461 (1979).
[14]J. Barbolla, S. Dueñas, and L. Bailón, Solid-State Electron. **35**(3), 285–297 (1992).
[15]J. Olea, G. González-Díaz, D. Pastor, I. Mártil, A. Martí, E. Antolín, and A. Luque. J. Appl. Phys. **109**, 063718 (2011).
[16]S. Dueñas, H. Castán, L. Enríquez, J. Barbolla, J. Montserrat, and E. Lora-Tamayo. Semicond. Sci. Technol. **9**, 1637–1648 (1994).